

---

---

# Strain-Based Mindlin Finite Element for Vibration Analysis of Rectangular Plates Coupled with a Fluid

**Faiçal BOUSSEM**

*Department of Hydrocarbons and Renewables Energies, Adrar University, ALGERIA,  
boussef-faiçal@univ-adrar.edu.dz*

**Abderahim BELOUNAR**

*Department of Civil Engineering, Tipaza University Center, Tipaza, ALGERIA.  
belounarab@yahoo.fr*

**Lamine BELOUNAR**

*MN2I2S Laboratory, Faculty of Science and Technology, Biskra University, ALGERIA,  
belounarl@yahoo.com*

**Lahcene FORTAS**

*MN2I2S Laboratory, Faculty of Science and Technology, Biskra University, ALGERIA,  
Fortas.lahcene@gmail.com*

*Abstract:* - This paper presents an extension of the recently published quadrilateral finite element to analyze the free vibration of plates vibrating in air or interacting with the fluid. The previously proposed four-node element is based on the strain approach and the Reissner-Mindlin plate theory. The developed finite element, which contains the three essential external degrees of freedom at each of the four corner nodes, is based on assumed functions of the strain field that satisfy the compatibility equations. A comparison is presented with experimental and numerical data available in the literature to demonstrate the performance of the current element. The dynamic characteristics (natural frequencies and associated modes) of a rectangular plate simply supported or clamped totally submerged in water, a cantilever square plate, and a partially submerged vertical plate are numerically computed by the proposed element. The frequencies obtained by this element are of excellent accuracy compared to numerical, analytical, or experimental solutions from the literature.

*Keywords:* - Finite element method; fluid-solid interaction; strain approach; Mindlin plate theory; free vibration, rectangular plate.

---

## 1. INTRODUCTION

Various methods, such as approximate numerical methods, have been developed to perform dynamic analysis of rectangular plates [1]–[5]. Structures coupled with a fluid have a wide application in nuclear, marine, and naval engineering. Structure-fluid interaction appears systematically when a structure is in contact with a fluid.

The motion of the fluid particles generates a variation in pressure close to the structure, known as "coupling" between the two components of the physical system. The interaction of the structure with a fluid has a significant effect on its dynamic response. A considerable decrease in frequency is caused by the exchange of kinetic energy between the fluid and the structure [6].

Different studies have been carried out to analyze the vibrations of plates in contact with a fluid. Lindholm et al. [7] performed experimental research

on the vibrations of cantilever plates in air and water, and the results were compared to theoretical predictions based on simple beam theory and thin-plate theory. Fu and Price [8] studied the dynamic behavior of a vertical or horizontal cantilever plate totally or partially immersed in water. The interaction between a vibrating flexible cantilever square plate, which may be partially or totally submerged within the fluid, has been successfully described using a linear hydro-elasticity theory. Ergin and Uğurlu [9] utilized an approach based on the boundary integral equation method and the method of images to compute the dynamic properties (wet natural frequencies and related modes) of two distinct, partially submerged cantilever plates.

Furthermore, analytical and experimental methods have been widely applied [8]–[11]. A numerical analysis [6] was also carried out on the vibrations of the plates in the air or water. The mathematical model

for structure is based on the finite element method and Sanders's shell theory.

The studies mainly focused on the development of plate elements based on the Reissner-Mindlin plate theory, which considers the transverse shear deformation through the plate thickness. Reissner [12] initially proposed this theory for bending plates, and it was further developed by Mindlin [13]. But when Mindlin's plate elements are used to analyze thin plates, various difficulties can occur, such as the phenomenon of shear locking.

Therefore, many researchers have used the strain-based approach to develop efficient and effective finite elements and eliminate shear locking. The strain field of the finite element in this approach is assumed by a mathematical function that satisfies the compatibility equations, and the displacement field is derived by direct integration of the strain-displacement relations. The strain approach has been successfully used for static and vibration of plates [14]–[22]. However, according to the above literature, no studies have been undertaken on analyzing fluid coupled plate vibrations using the strain approach. The previous has motivated the authors to study the dynamic behavior of plates in water using a finite element [16] based on the strain approach and the Reissner-Mindlin plate theory. The performance of this element was tested by analyzing static, free vibration, and plate buckling problems.

This study aims to calculate the natural frequencies of rectangular plates vibrating in water using a four-node element based on assumed strain functions and the Reissner-Mindlin plate theory. This element, called SBQP (Strain Based Quadrilateral Plate), is based on linear functions for the different components of the strain field, which satisfy the compatibility equations.

Furthermore, this element contains three degrees of freedom ( $W$ ,  $\beta_x$ , and  $\beta_y$ ) per node. Several tests for plates with different boundary conditions are performed to verify the performance of the developed element (SBQP). All calculations were performed by a Matlab finite element code developed by the authors of this study.

## 2. FORMULATION OF PROPOSED FINITE ELEMENT

### 2.1. Derivation of the displacements field

Figure 1 shows the geometry of a quadrilateral element having three degrees of freedom, the displacement component along the thickness ( $W$ ), and two rotations  $\beta_x = \theta_y$  and  $\beta_y = -\theta_x$  at each of the four corner nodes. The strains in terms of the

displacements are given for Reissner-Mindlin plate elements:

$$\begin{aligned} \kappa_x &= \frac{\partial \beta_x}{\partial x}, \quad \kappa_y = \frac{\partial \beta_y}{\partial y}, \quad \kappa_{xy} = \left( \frac{\partial \beta_x}{\partial y} + \frac{\partial \beta_y}{\partial x} \right) \\ \gamma_{xz} &= \beta_x + \frac{\partial W}{\partial x}, \quad \gamma_{yz} = \beta_y + \frac{\partial W}{\partial y} \end{aligned} \quad (1)$$

The five strains, bending ( $\kappa_x$ ,  $\kappa_y$ , and  $\kappa_{xy}$ ) and transverse shear ( $\gamma_{xz}$  and  $\gamma_{yz}$ ), given in equation (1) cannot be considered independent, for they are in terms of the displacements  $W$ ,  $\beta_x$ , and  $\beta_y$ ; therefore they must satisfy the compatibility equations given as [14]:

$$\begin{aligned} \frac{\partial^2 \kappa_x}{\partial y^2} + \frac{\partial^2 \kappa_y}{\partial x^2} &= \frac{\partial^2 \kappa_{xy}}{\partial x \partial y}, \dots\dots\dots \\ \frac{\partial^2 \gamma_{xz}}{\partial x \partial y} - \frac{\partial^2 \gamma_{yz}}{\partial x^2} + \frac{\partial \kappa_{xy}}{\partial x} &= 2 \frac{\partial \kappa_x}{\partial y}, \quad (2) \\ \frac{\partial^2 \gamma_{yz}}{\partial x \partial y} - \frac{\partial^2 \gamma_{xz}}{\partial y^2} + \frac{\partial \kappa_{xy}}{\partial y} &= 2 \frac{\partial \kappa_y}{\partial x} \dots\dots\dots \end{aligned}$$

The displacement field corresponding to the three rigid body modes is first calculated by equating equation (1) to zero and then integrating the resulting differential equations to obtain the displacement field.

$$W = \alpha_1 - \alpha_2 x - \alpha_3 y, \quad \beta_x = \alpha_2, \quad \beta_y = \alpha_3 \dots\dots (3)$$

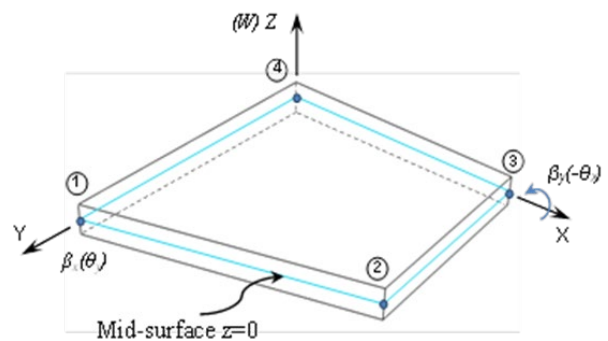


Figure 1. Quadrilateral plate finite element (SBQP)

The present quadrilateral element (SBQP) has three degrees of freedom ( $W$ ,  $\beta_x$ , and  $\beta_y$ ) at each node. Therefore, the displacements field should contain twelve independent constants. Three of them ( $\alpha_1$ ,  $\alpha_2$ ,  $\alpha_3$ ) are already used to represent the rigid body modes, and the remaining nine constants ( $\alpha_4$ ,  $\alpha_5$ , ...,  $\alpha_{12}$ ) are to be apportioned among the five assumed strains of the element. Therefore, the assumed strain

field for this finite element (SBQP) is given as follows[16]:

$$\begin{aligned} \kappa_x &= \alpha_4 + \alpha_5 y, & \kappa_y &= \alpha_6 + \alpha_7 x \\ \kappa_{xy} &= \alpha_8 + (2x)\alpha_5 + (2y)\alpha_7, & \gamma_{xz} &= \alpha_9 + \alpha_{10} y \\ \gamma_{yz} &= \alpha_{11} + \alpha_{12} x \end{aligned} \quad (4)$$

The terms in brackets of the assumed strains (equation (4)) are added to satisfy compatibility equations (equation (2)). The strain functions ( $k_x, k_y, k_{xy}, \gamma_{xz}, \gamma_{yz}$ ) given by equation (4) are substituted into equation (1), and after integration, we obtain:

$$\begin{aligned} W &= -\alpha_4 \frac{x^2}{2} - \alpha_5 \frac{x^2 y}{2} - \alpha_6 \frac{y^2}{2} - \alpha_7 \frac{xy^2}{2} - \alpha_8 \frac{xy}{2} + \alpha_9 \frac{x}{2} \\ &+ \alpha_{10} \frac{xy}{2} + \alpha_{11} \frac{y}{2} + \alpha_{12} \frac{xy}{2} \\ \beta_x &= \alpha_4 x + \alpha_5 xy + \alpha_7 \frac{y^2}{2} + \alpha_8 \frac{y}{2} + \alpha_9 \frac{1}{2} + \alpha_{10} \frac{y}{2} - \alpha_{12} \frac{y}{2} \\ \beta_y &= \alpha_5 \frac{x^2}{2} + \alpha_6 y + \alpha_7 xy + \alpha_8 \frac{x}{2} - \alpha_{10} \frac{x}{2} + \alpha_{11} \frac{1}{2} + \alpha_{12} \frac{x}{2} \end{aligned} \quad (5)$$

After combining the displacement functions obtained from equation (5) with the displacements of the rigid body modes defined in equation (3), the final displacement shape functions are obtained:

$$\begin{aligned} W &= \alpha_1 - \alpha_2 x - \alpha_3 y - \alpha_4 \frac{x^2}{2} - \alpha_5 \frac{x^2 y}{2} - \alpha_6 \frac{y^2}{2} - \alpha_7 \frac{xy^2}{2} \\ &- \alpha_8 \frac{xy}{2} + \alpha_9 \frac{x}{2} + \alpha_{10} \frac{xy}{2} + \alpha_{11} \frac{y}{2} + \alpha_{12} \frac{xy}{2} \\ \beta_x &= \alpha_2 + \alpha_4 x + \alpha_5 xy + \alpha_7 \frac{y^2}{2} + \alpha_8 \frac{y}{2} + \alpha_9 \frac{1}{2} + \alpha_{10} \frac{y}{2} - \alpha_{12} \frac{y}{2} \\ \beta_y &= \alpha_3 + \alpha_5 \frac{x^2}{2} + \alpha_6 y + \alpha_7 xy + \alpha_8 \frac{x}{2} - \alpha_{10} \frac{x}{2} + \alpha_{11} \frac{1}{2} + \alpha_{12} \frac{x}{2} \end{aligned} \quad (6)$$

The displacement and strain functions in equations (6) and (4) can be expressed in matrix form as:

$$\{U\} = [P]\{\alpha\} = [N]\{q_e\} \quad (7)$$

$$\{\varepsilon\} = [Q]\{\alpha\} = [B]\{q_e\} \quad (8)$$

where

$$[N] = [P][C]^{-1}, [B] = [Q][C]^{-1} \quad (9)$$

and the matrices  $[P]$ ,  $[Q]$ , and  $[C]$  are given in the appendix.

The displacements field, the strains field, and constant parameters vectors are:

$$\begin{aligned} \{U\} &= \{W, \beta_x, \beta_y\}^T, \{\varepsilon\} = \{\kappa_x, \kappa_y, \kappa_{xy}, \gamma_{xz}, \gamma_{yz}\}^T, \\ \{\alpha\} &= \{\alpha_1, \alpha_2, \dots, \alpha_{12}\}^T \end{aligned} \quad (10)$$

The element stiffness and mass matrices ( $[K^e]$ ,  $[M^e]$ ), are respectively as:

$$\begin{aligned} [K^e] &= \int_{S_e} [B]^T [D][B] dS \\ [K^e] &= [C]^{-T} \left( \int [Q]^T [D][Q] \det(J) d\xi d\eta \right) [C]^{-1} \quad (11) \end{aligned}$$

$$\begin{aligned} [M^e] &= \int_{S_e} [N]^T [T][N] dS \\ [M^e] &= [C]^{-T} \left( \int [P]^T [T][P] \det(J) d\xi d\eta \right) [C]^{-1} \quad (12) \end{aligned}$$

Where  $[D]$  and  $[T]$  are, respectively, rigidity, and the matrix containing the mass material density

The matrices  $[K_0]$  and  $[M_0]$  given in equations (11) and (12) are numerically computed with exact Gauss integration for quadrilateral element (SBQP).

## 2.2. Fluid formulation

The following assumptions simulate the fluid's dynamic behavior: the vibrations have small amplitude, and the fluid is incompressible, inviscid, and irrotational.

The force vector caused by the fluid can be expressed in the local reference X, Y, and Z as follows:

$$\{F\}^e = \int_S [R][C]^{-1} \{P\} dS \quad (13)$$

$[C]$  is the transformation matrix;

$[R]$  is a matrix of order  $(3 \times 12)$  given in the appendix.

$\{P\}$  is a vector containing the pressure applied by the fluid on the finite element.

$$\{P\} = Z_{fi} [R][C]^{-1} \left\{ \ddot{\delta} \right\} \quad (14)$$

The  $Z_{fi}$  coefficients depend on the fluid-structure contact model.

Placing equation (14) into equation (13), we obtain the fluid force vector as follows:

$$\{F\}^e = Z_{fi} \int_S [C]^{-T} [R]^T [R][C]^{-1} dS \left\{ \ddot{\delta} \right\}^e \quad (15)$$

$$\{F\}^e = [M_f]^e \left\{ \ddot{\delta} \right\}^e$$

Then we have:

$$[M_f]^e = Z_{fi} [C]^{-T} \int_S [R]^T [R] dS [C]^{-1} \quad (16)$$

where  $[M_f]^e$  is the added elementary mass matrix caused by the fluid.

The global system of equations of motion for a rectangular plate in contact with the fluid is:

$$[[M_s] - [M_f]] \{\ddot{\delta}_T\} + [K_s] \{\delta_T\} = \{0\} \quad (17)$$

$[M_s]$  and  $[K_s]$  are the mass and stiffness matrices of the plate without fluid, respectively;

$[M_f]$  is the global mass matrix representing the effect of the fluid inertial forces;

$\{\delta_T\}$  is the global displacements' vector.

The frequencies and vibration modes of the coupled fluid-structure system can be obtained by solving the eigenvalue problem expressed by:

$$\text{Det}[[K_s] - \omega^2 [M_s - M_f]] = 0 \quad (18)$$

### 3. NUMERICAL APPLICATIONS

#### 3.1. Rectangular plate totally submerged in water

A rectangular steel plate totally submerged in water is simply supported or clamped on two short sides (Figure 2). This test has been studied experimentally by Haddara and Cao [10]. The plate dimensions are length  $B=0.655$  m, width  $A=0.20165$  m, and plate thickness  $h=9.36$  mm.

The experimental installation was carried out by placing the plate in a rectangular tank of dimensions  $1.3\text{m} \times 0.55\text{m} \times 0.8\text{m}$ . The mechanical properties of this plate are solid density  $\rho_s=7850$  kg/m<sup>3</sup>, Poisson's ratio  $\nu=0.3$ , and Young's modulus  $E=207$  GPa. The fluid density is taken to be  $\rho_f=1000$  kg/m<sup>3</sup>.

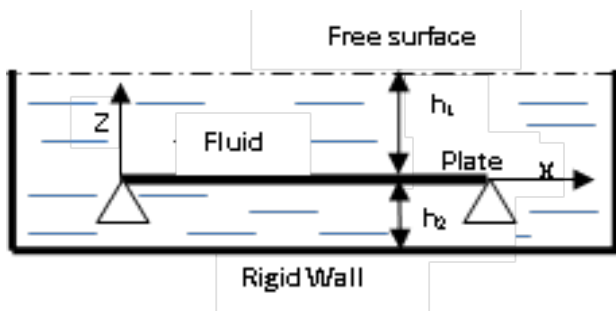


Figure 2. Rectangular plate totally submerged in water.

The dynamic pressure for this case is determined as [6] :

$$P = -\frac{\rho_f}{\mu} \left[ \frac{1 + Ce^{2\mu h_1}}{1 - Ce^{2\mu h_1}} + \frac{e^{-2\mu h_2} + 1}{e^{-2\mu h_2} - 1} \right] \frac{\partial^2 W}{\partial t^2} = Z_{fi} \frac{\partial^2 W}{\partial t^2} \quad (19)$$

$$\text{with } \mu = \pi \sqrt{\frac{1}{A^2} + \frac{1}{B^2}}$$

The value of  $C$  tends to  $-1$ . This approximation is made to avoid having a nonlinear eigenvalue system [6].

The natural frequencies (Hz) of the SBQP element with a mesh size of 288 elements are presented in Figure 3. Figures 4 and 5 show the first three vibration modes for a simply supported and clamped plate totally submerged in water.

These results of the present element for a given mesh are satisfactory compared to the numerical values of the finite rectangular element of Kerboua et al. [6], which has four nodes, each node has six degrees of freedom and compared to the experimental results of Haddara and Cao [10].

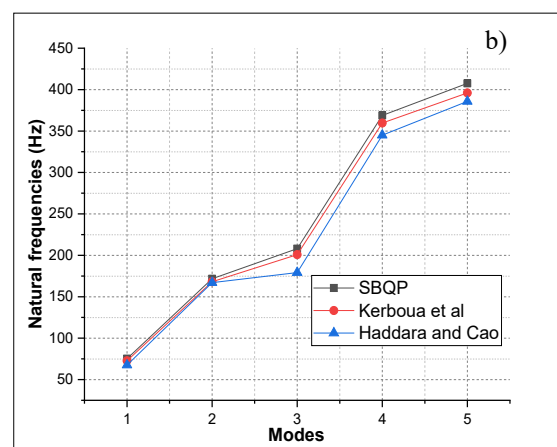
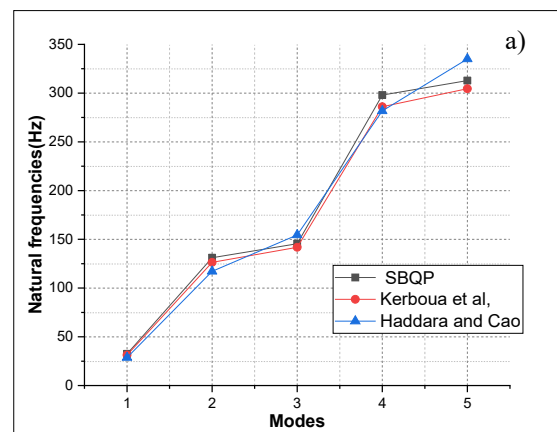


Figure 3. Natural frequency variation of horizontal plate totally submerged in water, a) simply supported, b) clamped plate

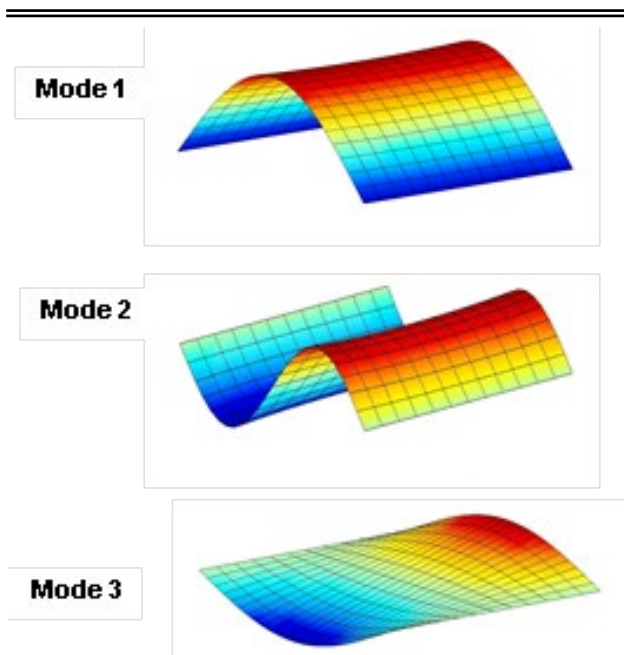


Figure 4. The first three vibration modes of the horizontal simply supported plate totally submerged in water

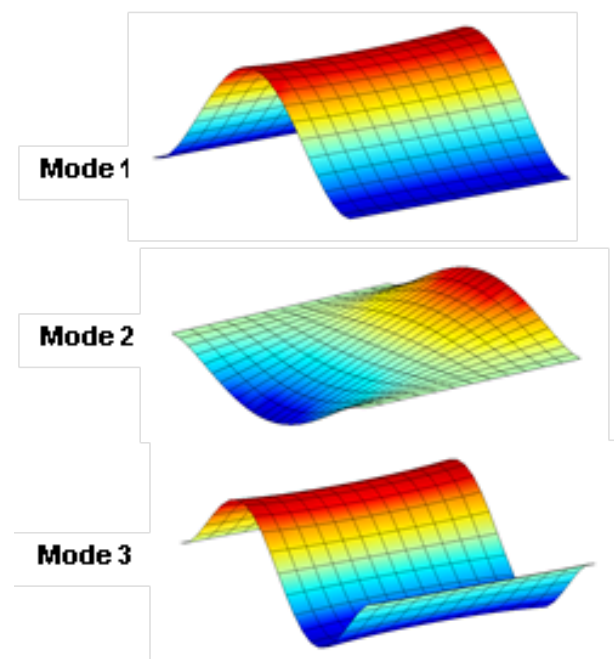


Figure 5. The first three vibration modes of the horizontal clamped plate totally submerged in water.

### 3.2. Cantilever square plate submerged in water

In this example, a square steel plate is clamped on one side only, totally submerged in a reservoir (Figure 6).

The dimensions and mechanical properties of the plate are  $A=B=10$  m and thickness  $h=0.238$  m.

The density of the solid  $\rho_s=7830$  kg/m<sup>3</sup>, Poisson's ratio  $\nu=0.3$ , and Young's modulus  $E=206$  GPa.

The water under the plate is assumed to be high

enough ( $h_2 \gg \text{length of the plate}$ ) not to affect the dynamic behavior of the coupled system [10]. This plate has been studied experimentally by Lindholm et al. [7] and numerically by Fu and Price [8] and Kerboua et al. [6].

The dynamic pressure for this case is determined as [6] :

$$P = -\frac{\rho_f}{\mu} \left[ \frac{1 + Ce^{2\mu h_1}}{1 - Ce^{2\mu h_1}} + \frac{e^{-2\mu h_2} + 1}{e^{-2\mu h_2} - 1} \right] \frac{\partial^2 W}{\partial t^2} = Z_{f_i} \frac{\partial^2 W}{\partial t^2} \quad (20)$$

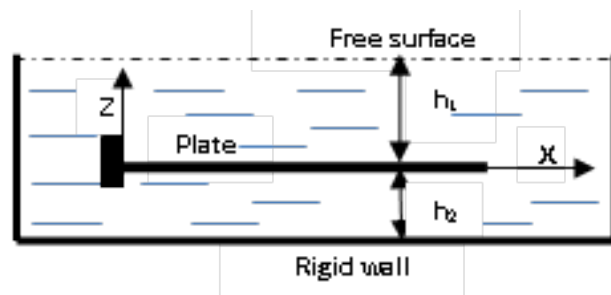


Figure 6. Cantilever square plate submerged in water.

The results obtained by the SBQP element with a mesh size of 144 elements are shown in Tables 3 and 4.

The mode shapes shown in Figure 7 correspond to the first three wet natural frequencies.

As can be seen, the results obtained from the present 4-node SBQP element agree well with those obtained from Kerboua et al. [6] element and other reference solutions.

Table 3. Natural frequencies  $\omega$  (rad/sec) of the square plate in vacuum.

Modes	Plate in vacuum		
	Present element	Kerboua et al[6]	Fu and Price[8]
1	12.84	12.93	12.94
2	31.42	31.69	31.93
3	79.25	79.37	79.8

Table 4. Natural frequencies  $\omega$  (rad/sec) of the square plate clamped on one side totally submerged in water ( $h_1=5$ ).

Modes	Plate submerged in water			
	Present element	Kerboua et al [6]	Fu and Price [8]	Lindholm [7]
1	6.97	7.0	7.35	6.56
2	17.07	17.16	20.19	19.66
3	43.05	42.98	50.11	45.32

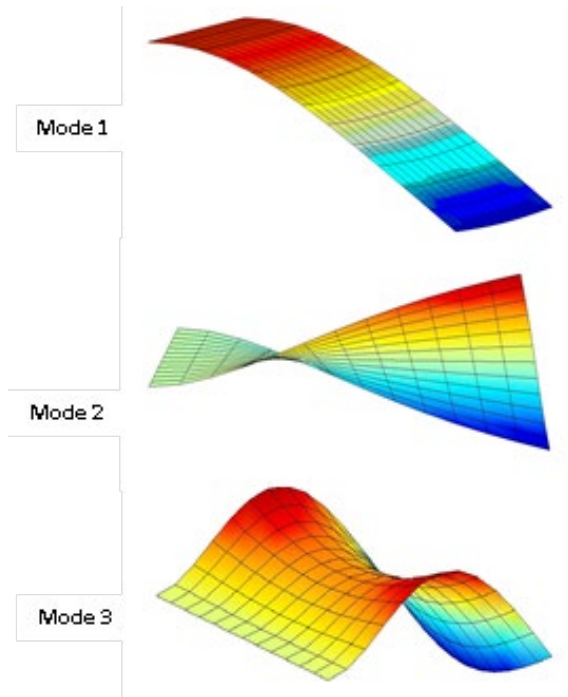


Figure 7. The first three vibration modes of the square plate clamped on one side totally submerged in water ( $h_1=5$ .)

### 3.3. Vertical plate partially submerged in water

Vertical plates submerged in a fluid reservoir behave differently than horizontal plates because the submerged finite elements are exposed to the fluid's pressure, while the dry components vibrate in a vacuum (Figure 8). The plate dimensions are length  $A=1.016$  m, width  $B=0.2032$  m, and thickness of the plate  $h=4.84$  mm. The mechanical properties of this plate are solid density  $\rho_s = 7830$  kg/m<sup>3</sup>, Poisson's ratio  $\nu=0.3$ , and Young's modulus  $E=206.8$  GPa. The density of the fluid is  $\rho_f=1000$  kg/m<sup>3</sup>.

The dynamic characteristics in the vacuum of the vertical plate have been studied. Table 5 shows the experimental results of Lindholm et al. [7] and the natural frequencies calculated by ANSYS (Ergin et al. [9]) and by the SBQP element for the first six modes. The results of the SBQP element (512 elements) are very close to the experimental measurements of Lindholm et al. [7]. The vibration analysis was carried out at four different degrees of immersion (25%, 50%, 75%, and 100%). The pressure of the fluid applied on the immersed part of the plate is equal to twice of the pressure expressed by the following equation [6]:

$$P = -\frac{\rho_f}{\mu} \left[ \frac{e^{-2\mu h_1} + 1}{e^{-2\mu h_1} - 1} \right] \frac{\partial^2 W}{\partial t^2} = Z_{f_1} \frac{\partial^2 W}{\partial t^2} \quad (21)$$

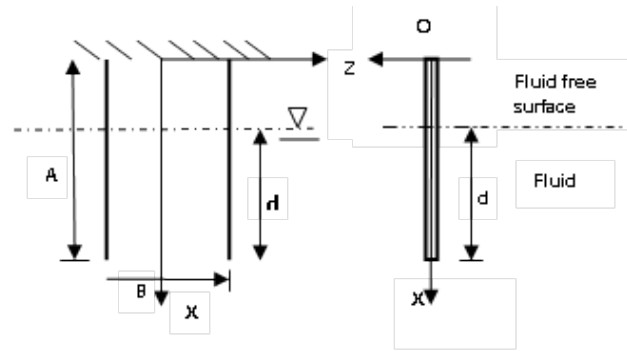


Figure 8. A vertical plate partially submerged in water.

Table 5. The first six modes of a vertical plate (in vacuum).

Modes	ANSYS 512 elements	Present element 512 elements	Lindholm[7]
1	3.94	3,943	3.84
2	24.66	24,682	24.20
3	39.07	39,360	39.10
4	69.24	69,268	68.10
5	119.47	120,397	121.00
6	136.35	136,235	-

The natural frequencies corresponding to the first two modes computed for various immersion levels are shown in Figure 9

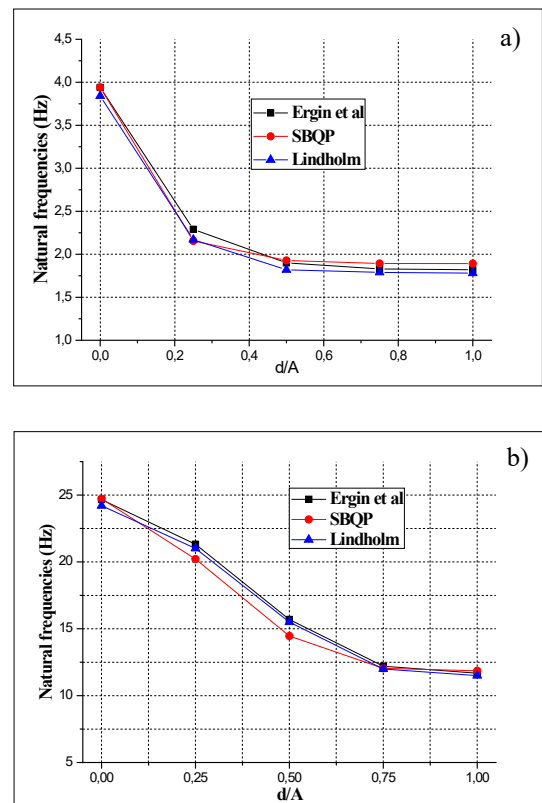


Figure 9. Natural frequency variation of a partially submerged vertical plate in a fluid as a function of the ratio ( $d/A$ ): (a) first mode, (b) second mode



It can be observed that the wet natural frequencies decrease as the  $d/A$  values increase, as depicted in Figure 9. The results obtained by the present four-node element SBQP are in good agreement with those obtained by Lindholm et al. [7] and Ergin et al. [9]. Figure 10 shows the first three vibration modes for a vertical plate partially submerged in water.

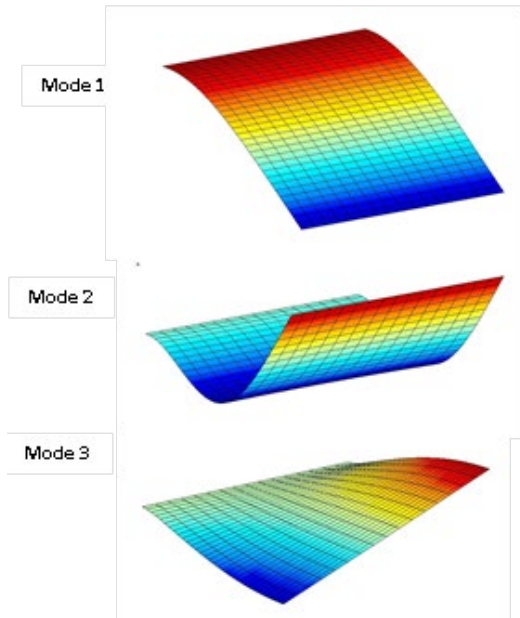


Figure 10. The first three vibration modes of the vertical plate partially submerged in water.

## 4. CONCLUSIONS

This paper aims to verify the performance of the existing finite element to describe the dynamic behavior of rectangular plates in contact with a fluid. The current four-node finite element (SBQP) has been developed using the strain approach and the Reissner-Mindlin plate theory.

This finite element possesses three usual degrees of freedom at each node. The structural mass and stiffness matrices were determined by numerical integration. Detailed numerical tests evaluated the efficiency of the proposed plate element on the free vibration analysis of thin plates in water.

The frequencies obtained by this element are of acceptable accuracy compared to numerical, analytical, or experimental solutions. Furthermore, the proposed finite element is free of shear locking and provides excellent results for the dynamic analysis of thin plates coupled with the fluid.

Overall, the present finite element has proven its efficiency and success in solving various fluid-structure interaction problems.

## APPENDIX

$$[P] = \begin{bmatrix} 1 & -x & -y & -\frac{x^2}{2} & -\frac{x^2 y}{2} & -\frac{y^2}{2} & -\frac{xy^2}{2} & -\frac{xy}{2} & \frac{x}{2} & \frac{xy}{2} & \frac{y}{2} & \frac{xy}{2} \\ 0 & 1 & 0 & x & xy & 0 & \frac{y^2}{2} & \frac{y}{2} & \frac{1}{2} & \frac{y}{2} & 0 & -\frac{y}{2} \\ 0 & 0 & 1 & 0 & \frac{x^2}{2} & y & xy & \frac{x}{2} & 0 & -\frac{x}{2} & \frac{1}{2} & \frac{x}{2} \end{bmatrix}$$

$$[Q] = \begin{bmatrix} 0 & 0 & 0 & 1 & y & 0 & 0 & 0 & 0 & 0 & 0 & 0 \\ 0 & 0 & 0 & 0 & 0 & 1 & x & 0 & 0 & 0 & 0 & 0 \\ 0 & 0 & 0 & 0 & (2x) & 0 & (2y) & 1 & 0 & 0 & 0 & 0 \\ 0 & 0 & 0 & 0 & 0 & 0 & 0 & 0 & 1 & y & 0 & 0 \\ 0 & 0 & 0 & 0 & 0 & 0 & 0 & 0 & 0 & 0 & 1 & x \end{bmatrix}$$

The transformation matrix  $[C]$  is given as:  $[C] = [[P_1] \ [P_2] \ [P_3] \ [P_4]]^T$

And the matrix  $[P_i]$  calculated for each of the four element nodes coordinates  $(x_i, y_i)$ ,  $(i=1,2,3,4)$  to obtain:

$$[P_i] = \begin{bmatrix} 1 & -x_i & -y_i & -\frac{x_i^2}{2} & -\frac{x_i^2 y_i}{2} & -\frac{y_i^2}{2} & -\frac{x_i y_i^2}{2} & -\frac{x_i y_i}{2} & \frac{x_i}{2} & \frac{x_i y_i}{2} & \frac{y_i}{2} & \frac{x_i y_i}{2} \\ 0 & 1 & 0 & x_i & x_i y_i & 0 & \frac{y_i^2}{2} & \frac{y_i}{2} & \frac{1}{2} & \frac{y_i}{2} & 0 & -\frac{y_i}{2} \\ 0 & 0 & 1 & 0 & \frac{x_i^2}{2} & y_i & x_i y_i & \frac{x_i}{2} & 0 & -\frac{x_i}{2} & \frac{1}{2} & \frac{x_i}{2} \end{bmatrix}$$

The matrix  $[R]$  is given as:

$$[R] = \begin{bmatrix} 1 & -x & -y & -\frac{x^2}{2} & -\frac{x^2 y}{2} & -\frac{y^2}{2} & -\frac{xy^2}{2} & -\frac{xy}{2} & \frac{x}{2} & \frac{xy}{2} & \frac{y}{2} & \frac{xy}{2} \\ 0 & 0 & 0 & 0 & 0 & 0 & 0 & 0 & 0 & 0 & 0 & 0 \\ 0 & 0 & 0 & 0 & 0 & 0 & 0 & 0 & 0 & 0 & 0 & 0 \end{bmatrix}$$

## REFERENCES

- [1] M. Tufoi, C. Hațiegan, O. Vasile, and G. R. Gillich, "Dynamic Analysis of Thin Plates with Defects by Experimental and FEM Methods," *Romanian Journal of Acoustics and Vibration*, vol. 10, no. 2, pp. 83–88, 2013
- [2] M. Tufoi, G. R. Gillich, I. C. Mituletu, and C. Hatiegan, "An analysis of the dynamic behavior of rectangular plates from a damage detection method," *Romanian Journal of Acoustics and Vibration*, vol. 12, no. 2, pp. 146–150, 2015
- [3] A. Belounar, F. Boussem, and A. Tati, "A Novel C0 Strain - Based Finite Element for Free Vibration and Buckling Analyses of Functionally Graded Plates," *Journal of Vibration Engineering & Technologies*, 2022, doi: 10.1007/s42417-022-00577-x
- [4] A. Belounar, F. Boussem, M. N. Houhou, A. Tati, and L. Fortas, "Strain-based finite element formulation for the analysis of functionally graded plates," *Archive of Applied Mechanics*, vol. 92, no. 7, pp. 2061–2079, 2022, doi: 10.1007/s00419-022-02160-y
- [5] A. Belounar, L. Belounar, and A. Tati, "An assumed strain finite element for composite plates analysis," *International Journal of Computational Methods*, 2022, doi: 10.1142/S0219876222500347
- [6] Y. Kerboua, A. A. Lakis, M. Thomas, and L. Marcouiller, "Vibration analysis of rectangular plates coupled with fluid," *Applied Mathematical Modelling*, vol. 32, no. 12, pp. 2570–2586, 2008, doi: 10.1016/j.apm.2007.09.004
- [7] U. Lindholm, D. Kana, W. Chu, and H. Abramson, "Elastic Vibration Characteristics of Cantilever Plates in Water," *Journal of Ship Research*, vol. 9, no. 02, pp. 11-36, 1965, <https://doi.org/10.5957/jsr.1965.9.2.11>
- [8] Y. Fu and W. G. Price, "Interactions between a partially or totally immersed vibrating cantilever plate and the surrounding fluid," *Journal of Sound and Vibration*, vol. 118, no. 3, pp. 495–513, 1987, doi: 10.1016/0022-460X(87)90366-X.
- [9] A. Ergin and B. Uğurlu, "Linear vibration analysis of cantilever plates partially submerged in fluid," *Journal of Fluids and Structures*, vol. 17, no. 7, pp. 927–939, 2003, doi: 10.1016/S0889-9746(03)00050-1
- [10] M. R. Haddara and S. Cao, "A Study of the Dynamic Response of Submerged Rectangular Flat Plates," *Marine Structure*, vol. 9, pp. 913–933, 1996. doi.org/10.1016/0951-8339(96)00006-8
- [11] C. C. Liang, C. C. Liao, Y. S. Tai, and W. H. Lai, "The free vibration analysis of submerged cantilever plates," *Ocean Engineering*, vol. 28, no. 9, pp. 1225–1245, 2001, doi: 10.1016/S0029-8018(00)00045-7
- [12] E. Reissner, "The Effect of Transverse Shear Deformation on the Bending of Elastic Plates," *Journal of Applied Mechanics*, vol. 12, pp. 69–77, 1945, doi.org/10.1115/1.4009435
- [13] R. D. Mindlin, "Influence of rotatory inertia and shear on flexural motion of isotropic, elastic plates," *J. Appl. Mech.*, vol. 18, pp. 31–38, 1955, doi.org/10.1115/1.4010217
- [14] L. Belounar and M. Guenfoud, "A new rectangular finite element based on the strain approach for plate bending," *Thin-Walled Structures*, vol. 43, no. 1, pp. 47–63, 2005, doi: 10.1016/j.tws.2004.08.003.
- [15] L. Belounar and K. Guerraiche, "A new strain based brick element for plate bending," *Alexandria Engineering Journal*, vol. 53, no. 1, pp. 95–105, 2014, doi: 10.1016/j.aej.2013.10.004.
- [16] A. Belounar, S. Benmebarek, M. N. Houhou, and L. Belounar, "Static, free vibration, and buckling analysis of plates using strain-based Reissner–Mindlin elements," *International Journal of Advanced Structural Engineering*, vol. 11, no. 2, pp. 211–230, 2019, doi: 10.1007/s40091-019-0226-4
- [17] F. Boussem, A. Belounar, and L. Belounar, "Assumed strain finite element for natural frequencies of bending plates," *World Journal of Engineering*, Vol. 19 No. 5, pp. 620-631, 2021, doi: 10.1108/WJE-02-2021-0114
- [18] F. Boussem and L. Belounar, "A Plate Bending Kirchhoff Element Based on Assumed Strain Functions," *Journal of Solid Mechanics*, vol. 12, no. 4, pp. 935–952, 2020, doi: 10.22034/jsm.2020.1901430.1601.
- [19] A. Belounar, S. Benmebarek, M. N. Houhou, and L. Belounar, "Free Vibration with Mindlin Plate Finite Element Based on the Strain Approach," *Journal of The Institution of Engineers (India): Series C*, vol. 101, no. 2, pp. 331–346, 2020, doi: 10.1007/s40032-020-00555-w
- [20] F. Boussem and L. Belounar, "A Plate Bending Kirchhoff Element Based on Assumed Strain Functions," *Journal of Solid Mechanics*, vol. 12, no. 4, pp. 935–952, 2020, doi: 10.22034/jsm.2020.1901430.1601
- [21] A. Messai, L. Belounar, and T. Merzouki, "Static and free vibration of plates with a strain based brick element," *European Journal of Computational Mechanics*, vol. 00, no. 00, pp. 1–21, 2018, doi: 10.1080/17797179.2018.1560845
- [22] A. Belounar, S. Benmebarek, and L. Belounar, "Strain based triangular finite element for plate bending analysis," *Mechanics of Advanced Materials and Structures*, vol. 27, no. 8, pp. 620–632, 2018, doi: 10.1080/15376494.2018.1488310